Bax Forms Two Types of Channels, One of Which Is Voltage-Gated

Shang H. Lin, Meenu N. Perera, Toan Nguyen, Debra Datskovskiy, Megan Miles, and Marco Colombini*
Department of Biology, University of Maryland, College Park, Maryland

ABSTRACT When activated, the proapoptotic protein Bax permeabilizes the mitochondrial outer membrane, allowing the release of proteins into the cytosol and thus initiating the execution phase of apoptosis. When activated Bax was reconstituted into phospholipid membranes, we discovered a new, to our knowledge, property of Bax channels: voltage gating. We also found that the same Bax sample under the same experimental conditions could give rise to two radically different channels: Type A, which is small, well behaved, homogeneous, and voltage-gated, and Type B, which is large, noisy, and voltage-independent. One Type B channel can be converted irreversibly into a population of Type A channels by the addition of La^{3+}. This conversion process appears to involve a two-dimensional budding mechanism. The existence of these two types of Bax channels suggests a process for controlling the degree of mitochondrial outer membrane permeabilization.

INTRODUCTION

Despite being a soluble cytosolic protein, Bax can undergo conformational changes to form transmembrane channels in the mitochondrial outer membrane, permeabilizing it and thus releasing a number of proteins, including cytochrome *c*, to trigger the execution phase of apoptosis. As a member in the Bcl-2 family of proteins, Bax plays a crucial role in promoting apoptosis. The Bcl-2 family proteins are characterized by having at least one of the four Bcl-2 homology domains (BH1–BH4). The consensus in the field is that there are three groups of proteins in the Bcl-2 family (1): proapoptotic pore-forming (e.g., Bax and Bak), antiapoptotic (e.g., Bcl-2 and Bcl-xL), and the proapoptotic BH3-only proteins (e.g., Bid and Bim). When they receive proapoptotic signals, the BH3-only proteins work either directly (2–4) or indirectly (5,6) on the pore-forming proteins to control the onset of apoptosis. This results in Bax monomers changing from being cytosolic proteins to oligomers in the mitochondrial outer membrane. Despite its obvious importance, the detailed mechanism of how this oligomerization occurs is still unclear. Questions such as how monomeric Bax forms the active oligomer, what conformational changes Bax undergoes, how Bax interacts with other Bcl-2 family proteins, and many others are still under study. Due to the difficulties of solving the structure of membrane proteins in a membrane environment, investigators have employed many indirect approaches to address these questions (7–9), resulting in different models of the membrane structure of Bax oligomers. Based on electron paramagnetic resonance (EPR) results, Bleicken et al. (10) proposed that spin-labeled reconstituted Bax forms dimers through the BH3 domain to nucleate the subsequent oligomerization. Another group (11) found that Bax monomers first interact with each other through the BH1-3 domain, and this then triggers the conformational change of the rear pocket of Bax to cause further oligomerization. Experiments with mutants of Bax expressed in knockout mice (12) indicated that only BH1 and BH3 are responsible for oligomerization in the membrane. These insights and others will eventually yield an understanding of the steps that lead to the formation of Bax channels in the mitochondrial outer membrane (13,14). Here, we pursue a reductionist approach by examining the electrophysiological properties of channels formed by Bax in planar phospholipid membranes, and thus gain insights into their permeability properties and dynamics.

Channels formed in a planar membrane system by Bax lacking the transmembrane domain were first studied in 1997 by Antonsson et al. (15) and Schlesinger et al. (16). The former group found that the channel activity was enhanced when negative potential was applied at the same side Bax added, indicating an intrinsically asymmetric channel formation. Under symmetric solutions of 125 mM NaCl, the conductance recorded showed elementary channels of 5.6 ± 0.2 pS increasing to 26 ± 7 pS, and then fluctuating between this level and 250 ± 25 pS (15). Schlesinger et al. (16) reported that Bax-induced conductances showed transitions among three different conductance levels: a closed state and two conductance levels. Their experiments were performed in the presence of a salt gradient (450/150 mM KCl) and indicated an anion-selective conductance ($P_K/P_{Cl} = 0.32$) (16,17). The Antonsson group reported a preference for cations ($P_{Na}/P_{Cl} = 2$). The conductance observed by Schlesinger and co-workers showed mild outward rectification in symmetrical 150 mM KCl along with rapid flickering at 70 mV and periodic closure at −70 mV.

In studies with full-length Bax in the same system, Basañez and co-workers (18) observed that the formation of conductances was quickly followed by membrane instability (membranes usually ruptured after some tens of minutes, or even fewer when the concentration of Bax was ~1 nM,

Submitted June 22, 2011, and accepted for publication September 20, 2011.

*Correspondence: colombini@umd.edu

Editor: Robert Nakamoto.

0006-3495/11/11/2163/7 $2.00

doi: 10.1016/j.bpj.2011.09.041

with voltage held at 40 mV). The authors demonstrated that added Bax induces measurable instability in planar membranes, reducing their ability to withstand high voltages. They proposed that Bax induces the formation of lipidic pores that are responsible for the release of proteins from mitochondria.

Investigators have used patch-clamping of mitochondrial membranes isolated from cells undergoing apoptosis or treated with Bax to study the electrophysiological behaviors of channels presumably formed by Bax. Jonas et al. (19) performed intracellular patch-clamping of squid mitochondria treated with Bax (both full-length and truncated) and found that the conductance of the channels that were formed did not comprise multiples of a single unitary conductance, and there was no consistent major conductance level. Martinez-Caballero and co-workers (20) recorded channels in mitochondria from cells undergoing apoptosis and called them mitochondrial apoptosis-induced channels (MACs). They provided compelling evidence that these channels are due to the presence of either Bax or Bak. In symmetric media of 150 mM KCl, the MACs showed incremental steps around 300 pS that were voltage-independent and cation-selective.

Here we report results obtained with the use of full-length Bax that was activated with octyl-glucoside and reconstituted into planar phospholipid membranes. We found that Bax forms two types of channels with different characteristics. One of these channels is voltage-gated and closes asymmetrically at elevated potentials. The properties and dynamics of these channels point to possible roles in the apoptotic process.

MATERIALS AND METHODS

Materials

Diphytanoylphosphatidylcholine was purchased from Avanti Polar Lipids (Alabaster, AL). Cholesterol was obtained from Sigma (St. Louis, MO). Asolectin (polar extract of soybean phospholipids) was generated from lecithin type II-S (Sigma Chemical, St. Louis, MO) purified as described previously (21). Stock solutions of $LaCl_3$ used in these experiments were either 1 mM or 10 mM in distilled water.

Preparation of Bax

Recombinant full-length human Bax was made as previously described (22,23), and after elution from the chitin column (New England Biolabs, Ipswich, MA), it was dialyzed (12,000 MW cutoff) at 4°C first for 24 h against 3 liters of 1 mM EDTA and 20 mM Tris-HCl, pH 8.0, and then against 5 liters of 20 mM Tris-HCl, pH 8.0, for 24 h. The Bax was then supplemented with glycerol to 10% (v/v) and filtered sterilized through a 0.2 μm filter. Aliquots (generally 0.2 ml) were rapidly shell-frozen in ethanol and dry ice, and stored at <-80°C. The concentration of Bax was 10–35 μg/ml (depending on the preparation), as determined with a MicroBCA Protein Kit (Pierce Chemical). SDS/PAGE was used to test the purity of protein, and silver staining showed 95% of the stain in the monomeric Bax band. Because of its tendency to oligomerize over time in 4°C (24), the Bax was frozen immediately after purification and only thawed on ice right before use. No detergent was used in protein isolation or purification. To activate monomeric Bax, it was incubated with β-octyl glucoside of a final concentration of 0.7% (w/v) for at least 30 min on ice. The concentrations of activated Bax indicated in this work were based on the monomeric Bax (21 kDa) because the activated form is heterogeneous.

Electrophysiological recordings

Planar membranes were formed according to the modified monolayer method (25,26) across a hole (diameter of 100 μm) in a Saran partition after it was coated with petrolatum. For most experiments, the membrane-forming solution (0.5% (w/v) DPhPC, 0.5% (w/v) asolectin, and 0.05% (w/v) cholesterol in hexane) was layered on the surface of the aqueous solution (1.0 M KCl, 1 mM $MgCl_2$, and 5 mM PIPES, pH 6.9). For selectivity experiments, the concentration of KCl was reduced to 0.1 M on the grounded side. Reversal potentials were measured and permeability ratios calculated via the Goldman-Hodgkin-Katz equation (27,28). After hexane evaporation and monolayer formation were completed, the membrane was formed. Calomel electrodes with saturated KCl bridges were used to interface with the aqueous phase. The voltage was clamped and the current was recorded. In the text, we specify the number of experiments performed in which the particular observation was made. If all of the experiments yielded the same outcome, only the number of experiments is indicated. If only a subset of experiments yielded that result, we also specify the total number of experiments performed.

Calculation of channel diameter

Single-channel conductance measurements were converted to estimates of channel diameter as follows:

$$d = 0.5\frac{G}{\lambda} + \sqrt{\frac{G^2}{4\lambda^2} + \frac{4GL}{\lambda\pi}},$$

where d is the diameter of the channel, G is the conductance, λ is the conductivity, and L is the length of the channel (5 nm). This calculation assumes that the conductivity of the solution in the channel is the same as that of the bulk phase. The equation takes into consideration the access resistance as previously described (29).

RESULTS

Addition of full-length Bax into the aqueous phase of a planar phospholipid membrane (final concentration of Bax: ~10 nM) under voltage-clamped conditions results in one of two different types of conductance behavior (see details below). These are designated as Type A and Type B. The probability of the occurrence of Type A and Type B is ~50%. In most experiments, only one of the two types was observed. In very rare cases (probability: <5%), we observed a spontaneous change from Type A to Type B channels after new additions of Bax (but not vice versa).

Type A

Type A behavior has basically four characteristics: discrete, low-current-noise increments of conductance representing channel formation; voltage gating; and no change in conductance or voltage gating after addition of $LaCl_3$ (as opposed to the changes seen with Type B). After the

addition of activated Bax, the conductance increased in discrete and stepwise increments, with virtually no decrements (Fig. 1). These conductances had very low current noise in comparison with the Type B channels (vide infra). The total conductance achieved ranged from a few nanoSiemens to 100 nS, depending on the number of channels formed. The histogram of the insertion steps (Fig. 1, *inset*) appears to consist of three groups of conductances. These were fitted to three overlapping Gaussian curves. The fundamental unit seems to be the first Gaussian with a peak at 1.5 ± 0.4 nS. The peak of the second distribution at 4.1 ± 0.7 nS has a conductance ~3 times as great, hinting at the simultaneous insertion/formation of three units. The third peak is twice the second.

Type A Bax channels are voltage-gated. When the transmembrane voltage was raised above 60 mV, a population of uniform, low-noise step-wise drops in conductance was observed (Fig. 2). The histogram of these events shows a single peak at 1.4 nS (Fig. 2, *inset*), matching the value of the first peak in the insertion histogram. This indicates that the membrane conductance was due to many virtually identical channels. Reducing the voltage to 10 mV results in slow channel reopening (see Fig. S1 in the Supporting Material) and the rate of reopening slows further the longer the channels are closed. The slow kinetics and adaptation to the applied voltage do not allow the system to reach an equilibrium that would allow quantitation of the voltage-gating parameters.

In agreement with the Bax channels previously observed (15), the Type A channels are asymmetric because they only closed when the voltage of one sign was applied. The sign of the high voltage that could induce the drops in conductance varied from experiment to experiment with a frequency of

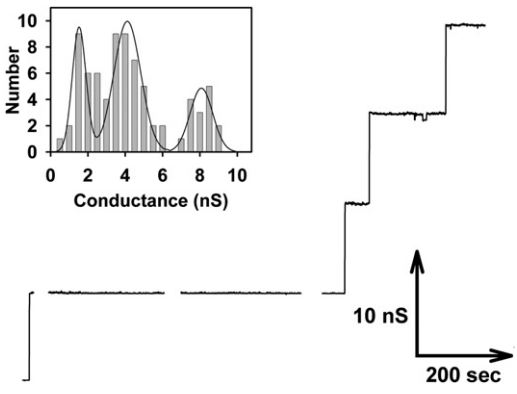

FIGURE 1 xformation of Type A Bax channels. The membrane conductance increased (starting from 0 nS) as a function of time after the addition of octylglucoside-activated Bax to the aqueous phase (1.0 M KCl on both sides of the membrane). The transmembrane voltage was clamped at 10 mV. The solution was stirred during the breaks in the record. The histogram of conductance increments from 16 separate experiments is shown in the inset. Only a few steps were larger than 10 nS and for clarity are not shown here. The histogram was fitted to three Gaussians with mean ± SD = 1.5 ± 0.4, 4.1 ± 0.7, and 8.1 ± 0.6.

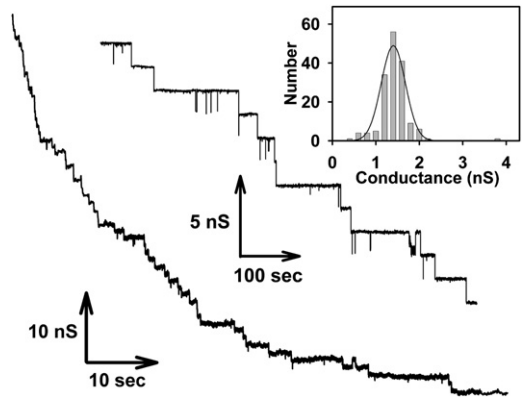

FIGURE 2 Voltage gating of Type A Bax channels. Stepwise conductance decrements were observed after the application of high voltage. The lower record is an example of an experiment with many Type A channels present in the membrane. The voltage was clamped at 70 mV. The upper record is an example of an experiment with fewer channels, with voltage held at 60 mV. The inset shows a histogram of the conductance decrements observed in 10 separate experiments (1.0 M KCl on both sides of the membrane). This distribution has a mean ± SD = 1.4 ± 0.3.

positive: negative = 13: 2. Thus, in most experiments the application of a positive potential on the side of the membrane to which Bax was added resulted in channel closure exclusively at positive potentials, demonstrating that all the channels were oriented in the same direction. This indicates that the channels are forming in a cooperative and oriented manner reminiscent of the autodirected insertion phenomenon first described for VDAC channels (30).

Addition of La^{3+} to the medium had no effect on the conductance or on the voltage dependence of the channels. This is important when considering the influence of La^{3+} on the Type B channels. Thus characteristics of discrete, low-noise conductance increments and voltage-dependent channel closure define what we refer to as Type A Bax channels.

Type B

In contrast to Type A, experiments that produced Type B conductance were characterized by indistinct conductance increases that included a great deal of current noise but were punctuated by some discrete increases of variable conductance. The conductance increased to a total value from 60 nS to a few hundred nanoSiemens before stabilizing. Even after it stabilized (i.e., with no net increase or decrease), the conductance fluctuated and continued to have excess current noise (Fig. 3 *A*). Unlike Type A, Type B conductance is voltage-independent (Fig. 3 *A*) at both positive and negative potentials. We applied transmembrane voltages as high as 120 mV without detecting any significant decrement or increment of conductance in these Type B experiments. These characteristics define the behavior of what we call Type B Bax channels. Because Type B channels are voltage-independent, there is no indication from these experiments as to whether the constituents of the

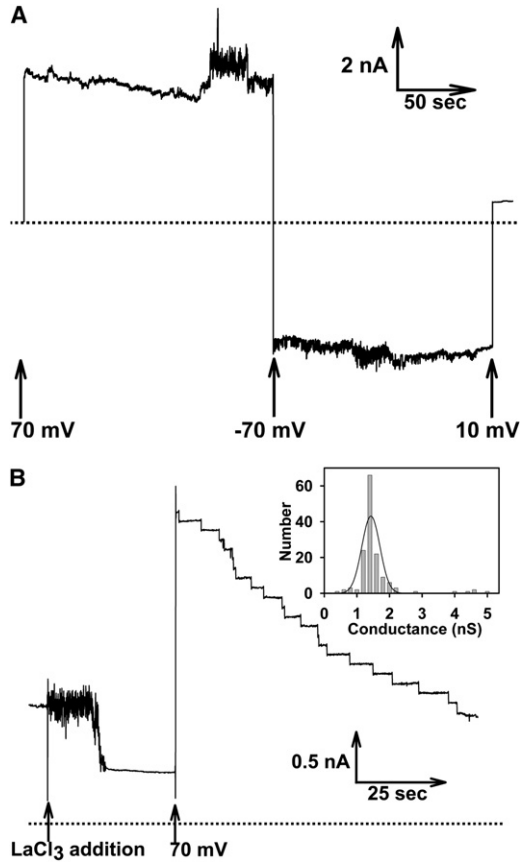

FIGURE 3 Conversion of a voltage-independent Type B Bax channel into a population of Type A channels. (*A*) Addition of Bax resulted in a noisy conductance increase. Neither +70 nor −70 mV caused any significant decrement in conductance. (*B*) The voltage was held at 10 mV before 70 mV was applied as indicated. The addition of $LaCl_3$ (8 μM) to this same membrane resulted in a conductance drop by a little more than half. The large fluctuations were due to the stirring motor. Application of 70 mV resulted in a population of uniformly sized, stepwise decrements. The inset is a histogram of conductance decrements collected from five separate experiments performed in the same way. The histogram was fitted to a Gaussian with mean ± SD = 1.4 ± 0.3. The dotted line designates the zero current level.

conductance in Type B experiments are due to many channels or just a single, huge channel.

Conversion from Type B to Type A

It has been shown that lanthanides can act on membranes to change the surface potential and lateral pressure. They can induce membrane fusion and regulate certain membrane channels (31–35). $LaCl_3$ affects Type A and Type B differently. $LaCl_3$ was added after the level of the conductance had reached a nearly constant value. It was added at a final concentration of a few μM on the same side of the chamber to which Bax had been added. Type A Bax channels showed neither a change in conductance ($n = 12$) nor a change of the voltage-gating behavior ($n = 4$) after $LaCl_3$ addition. However, for the Type B Bax channels, $LaCl_3$ addition resulted in a huge drop (85% ± 15% of original level) in conductance (Fig. 3 *b*). The drop was preceded by a variable delay time (8–113 s, $n = 14$; Fig. 4), characteristic of a stochastic process. Moreover, the residual conductance after the drop showed voltage gating ($n = 9$ out of 10) that was indistinguishable from the voltage gating of Type A Bax channels. Analysis of the step size of the decrements of the residual conductance under high voltage (Fig. 3, *inset*) shows the same pattern as that of de novo Type A (Fig. 2, *inset*). The stochastic behavior is consistent with a single large channel, but the residual conductance is composed of many channels. Therefore, we hypothesize that $LaCl_3$ helps to convert Type B into Type A Bax channels by means of a budding process. In analogy to vesicle budding from a membrane surface, a Type B channel undergoes lateral budding in two dimensions into many Type A channels.

The budding hypothesis is supported by a number of experimental and theoretical considerations. The stochastic delay before the conductance drop indicates that the drop involved a single structure, a single channel. This single structure may have been present along with the Type A channels, with the latter obscured by the properties of the former. However, the complete lack of voltage dependence is inconsistent with this alternative. Despite the noisy record, the voltage-dependent closure of Type A channels should have been detected. The La^{3+}-induced conductance drop did not have any detectable structure, i.e., there was no evidence of discrete closing events ($n = 14$). A budding process would be expected to result in a more fluid reduction in conductance rather than discrete drops in conductance. Finally, calculations made by using the conductance before La^{3+} addition, assuming one large channel, resulted in

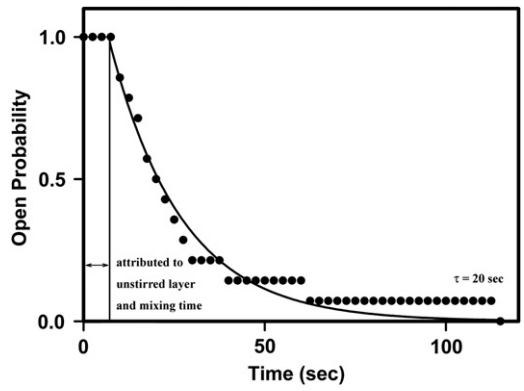

FIGURE 4 Summary of the time delay between the addition of $LaCl_3$ and the beginning of the drop of conductance. Each data point represents the fraction of experiments in which the conductance had not started to decrease at the specified time (the *x* axis) after $LaCl_3$ addition. Data were collected from 14 experiments. Only one experiment was performed in the presence of a KCl gradient (*cis* = 1.0 M, *trans* = 0.1 M), and this had a delay time of 10 s. All others were performed with 1.0 M KCl on both sides. The fitted line has a time constant of 20 s. The delay before the decay, attributed to the combination of diffusion time through the unstirred layer and time for mixing $LaCl_3$ into the solution, was 6.8 s.

a circumference that was greater than the sum of the circumferences of the channels that made up the residual conductance ($n = 13$). This is consistent with the budding hypothesis if some of the protein making up the circumference of the large channel formed the Type A channels, and some of it left the channel structure. The conversion of Bax protein into nonconducting structures was evident in one experiment in which the La^{3+}-induced conductance drop resulted in no residual conductance.

Measurement of the selectivity of Type A channels

The selectivity (P_K/P_{Cl}) of Type A Bax channels was determined in the presence of a gradient of KCl across the planar membrane (0.1 M and 1.0 M). The permeability ratio was 3.6 ± 0.3 (mean ± SD) and did not change after addition of $LaCl_3$ (3.7 ± 0.5; $n = 5$; Table 1). La^{3+} must not be binding in a region of Bax that is close to the ions flowing through the membrane. Also, by monitoring both selectivity and conductance at the same time, it is clear that the selectivity did not change with conductance increments or decrements ($n = 5$; Table 1). This supports the conclusion that Type A Bax channels do not merge with each other to form larger channels. All attempts to measure the selectivity of Type B channels failed, presumably because the Type B channels are unstable in the presence of an ion concentration gradient.

DISCUSSION

The reconstitution of full-length Bax that was isolated in a functional manner from the soluble fraction of a bacterial lysate into phospholipid membranes resulted in the formation of one of two types of channels. Type A is functionally homogeneous, with a distinct membrane orientation and a single voltage-gating process. The voltage gating resulted in channel closure at one sign of the membrane potential depending on the orientation of the population of channels. These channels show weak cation selectivity and a conductance consistent with a pore diameter of 0.9 nm. Type A channels are unlikely to be able to translocate proteins across membranes.

TABLE 1 Lack of variation in reversal potential with time, conductance, and La^{3+} addition

Before La^{3+}	After La^{3+}	*P*-value
−24 ± 1.5 mV	−24 ± 2.2 mV	0.96
Low conductance	High conductance	*P*-value
−24 ± 1.5 mV	−24 ± 1.8 mV	0.21
Early time	Late time	*P*-value
−25 ± 1.4 mV	−24 ± 2.0 mV	0.10

Reversal potentials of five separate Type A channel experiments were measured throughout the experiment, grouped, and compared to see whether any distinguishable changes in channel selectivity occurred before or after La^{3+} addition, between low or high conductance, and between the first half and second half of the experiment. Measurements were made in the presence of a KCl gradient (*cis* = 1.0 M, *trans* = 0.1 M), with the sign referring to the high salt side. Values are averages ± SD.

The voltage gating exhibited by the Type A channels is complex. Some of the complexity is attributed to kinetic delays, as is evident in the slow reopening process (Fig. S1). The system did not reach equilibrium during the time of the experiment and thus could not be fitted to a Boltzmann distribution. Thus, the typical voltage gating parameters—*n* (the number of charges that would need to traverse the membrane to account for the voltage dependence) and V_0 (the voltage at which half the channels are open)—could not be obtained. Furthermore, we suspect that closure is accompanied by some form of deoligomerization because channel reopening after voltage-dependent closure becomes incomplete if the high closure voltage is maintained for extended periods of time.

Type B channels seem to be large channels that are likely protein-permeable. Their conductance fluctuates with time, and they are voltage-independent. These channels seem to be unstable in the presence of an ion gradient and are rapidly converted to Type A channels after the addition of La^{3+} by what appears to be a process of channel budding in two dimensions. The delay before budding is stochastic, characteristic of a single structure undergoing the process. The transition has a time constant of 20 s ($n = 14$), consistent with an energy barrier of 80 kJ/mole.

The results reported here show some similarity to findings from other groups (15–17,20), but also major differences. To our knowledge, no one else has reported the large uniform populations of channels reported here. Conductance changes in the range of the conductance increments observed here for the insertion steps were observed when corrected for differences in salt concentration, but those channels had much higher flickering rates. There has been no report of voltage-gated channels formed by Bax; however, other investigators applied voltages up to 50 mV (20), which may be insufficient to observe significant channel closure. As for the selectivity, our measurements are similar to those obtained in a previous study of MACs (36), slightly more cation-selective than reported by one group for channels formed by truncated Bax (15), but opposite to the value (anion-selective) observed by another group (16). These differences (see also Westphal et al. (13)) may be explained by 1), the possibility that Bax forms different structures under different conditions; 2), the use of full-length versus truncated Bax; and 3), the quality of the Bax, including the mode of isolation and storage. In this work, we verified that the Bax was functional by testing its channel-forming ability on isolated mitochondria. When activated by either detergent or tBid, the activated Bax permeabilized the mitochondrial outer membrane to proteins (23).

The paucity of structural information makes it difficult to compare the channels reported here with those formed in isolated mitochondria. Evidence indicates that helices α5,

α6, and α9 of Bax are responsible for membrane insertion (10,37,38). Several possible models of active Bax oligomers in membrane have been reported. For example, it has been proposed that when the BH3 domain of Bax is activated by BH3-only proteins, it binds to the α1/α6 pocket of a second Bax monomer, and this activation propagates to other monomers, resulting in oligomerization (14). Others have provided evidence for a two-interface model wherein oligomerization occurs through two interacting surfaces: BH3:groove and α6:α6. Bax monomers first form dimers through a BH3 domain on one protein binding to the BH3-binding groove of another protein. The dimer now has two α6 helix regions and is therefore a divalent ligand. These oligomerize by binding to each other via their α6 helix domains (10,13). At present, there is insufficient evidence to enable a clear consensus. There is also no clear consensus on the number of Bax monomers that form the active structure (it varies from four (39), nine (20), or even >100 (40)). The reported size of the channels also varies from a few nanometers to ~27 nm depending on the system studied (2,39–41). Perhaps that is the nature of the Bax pore. The variable size of the Type B channel would be consistent with a variable number of Bax monomers forming the channel.

The histogram of conductance steps of voltage-gated closures of Type A channels (Fig. 2, *inset*) has a peak at 1.4 nS, and this is the same as the first peak of the insertion histogram (Fig. 1, *inset*). Higher conductance insertion events may represent the simultaneous insertion/formation of multiple channels at once. One can calculate the size of these channels by assuming cylindrical structures whose internal conductivity is the same as the bulk phase. The 1.4 nm decrements of Type A channels correspond to a diameter of 0.9 nm. This is smaller than the size of cytochrome *c* (~3.4 nm), an essential protein that is released from mitochondria after Bax is inserted into the outer membrane. However, the stochastic delay that occurs before the transformation of Type B into Type A suggests that each Type B conductance should be due to one structure, likely one channel. Although such structures would be variable in conductance, if they were formed by cylindrical channels, they would be very large (up to 40 nm) and thus very suitable for protein translocation. As for which domains of the Bax molecules are responsible for the voltage gating, our results combined with the previous models (10,11) suggest that it could be the charged residues on helix α5, which is transmembrane.

One can only speculate about the physiological relevance of our results. The instability of the Type B channels and conversion to Type A may indicate the presence of a regulatory mechanism. The ability of Bax channels to release proteins would be unstable, and thus they could be easily converted to protein-impermeable channels in response to an appropriate signal. This would not be La^{3+} but some other agent acting in a similar manner. Lanthanides inhibit the stretch-dependent opening of stretch-sensitive channels by acting on the membrane lipids and affecting the membrane tension. A similar action may be the trigger that causes the Type B channels to convert to Type A. The function of the voltage dependence is unclear; however, highly conserved voltage-gated channels (the VDAC channels) are found in all of the mitochondria tested. The mitochondrial outer membrane potential has been measured at ~30–40 mV (42–44), and theoretically it could increase to 60 mV (43). In addition, local electric fields, such as those resulting from surface charge, could act on the voltage sensor of the Type A channels, resulting in channel closure or disassembly. The physiological role, if any, of the asymmetrical orientation of Type A channels is unknown. However, according to Ausili et al. (45), the orientation of the C-terminus of Bax can be influenced by the lipid environment. Hence, the cooperative and variable orientation may serve some function, such as responding to the changing lipid composition of the outer membrane during apoptosis. Regardless of these issues, by using a reductionist approach in this work, we were able to identify novel (to our knowledge) properties of Bax channels that will provide insight into the structure and function of these channels.

SUPPORTING MATERIAL

Two figures are available at http://www.biophysj.org/biophysj/supplemental/S0006-3495(11)01132-5.

We thank Richard Youle for providing us with the plasmid of full-length Bax, and Brian Bujarski, Sajeela Padder, and Stephanie Fischer for assisting with the experiments on planar membranes.

This work was supported by a grant from the National Science Foundation (MCB-1023008).

REFERENCES

1. Youle, R. J., and A. Strasser. 2008. The BCL-2 protein family: opposing activities that mediate cell death. *Nat. Rev. Mol. Cell Biol.* 9:47–59.
2. Kuwana, T., M. R. Mackey, …, D. D. Newmeyer. 2002. Bid, Bax, and lipids cooperate to form supramolecular openings in the outer mitochondrial membrane. *Cell.* 111:331–342.
3. Letai, A., M. C. Bassik, …, S. J. Korsmeyer. 2002. Distinct BH3 domains either sensitize or activate mitochondrial apoptosis, serving as prototype cancer therapeutics. *Cancer Cell.* 2:183–192.
4. Kim, H., M. Rafiuddin-Shah, …, E. H. Cheng. 2006. Hierarchical regulation of mitochondrion-dependent apoptosis by BCL-2 subfamilies. *Nat. Cell Biol.* 8:1348–1358.
5. Willis, S. N., J. I. Fletcher, …, D. C. Huang. 2007. Apoptosis initiated when BH3 ligands engage multiple Bcl-2 homologs, not Bax or Bak. *Science.* 315:856–859.
6. Chen, L., S. N. Willis, …, D. C. Huang. 2005. Differential targeting of prosurvival Bcl-2 proteins by their BH3-only ligands allows complementary apoptotic function. *Mol. Cell.* 17:393–403.
7. Lalier, L., P.-F. Cartron, …, F. M. Vallette. 2007. Bax activation and mitochondrial insertion during apoptosis. *Apoptosis.* 12:887–896.
8. Gavathiotis, E., D. E. Reyna, …, L. D. Walensky. 2010. BH3-triggered structural reorganization drives the activation of proapoptotic BAX. *Mol. Cell.* 40:481–492.

9. Gavathiotis, E., M. Suzuki, …, L. D. Walensky. 2008. BAX activation is initiated at a novel interaction site. *Nature.* 455:1076–1081.
10. Bleicken, S., M. Classen, …, E. Bordignon. 2010. Molecular details of Bax activation, oligomerization, and membrane insertion. *J. Biol. Chem.* 285:6636–6647.
11. Zhang, Z., W. Zhu, …, J. Lin. 2010. Bax forms an oligomer via separate, yet interdependent, surfaces. *J. Biol. Chem.* 285:17614–17627.
12. George, N. M., J. J. D. Evans, and X. Luo. 2007. A three-helix homo-oligomerization domain containing BH3 and BH1 is responsible for the apoptotic activity of Bax. *Genes Dev.* 21:1937–1948.
13. Westphal, D., G. Dewson, …, R. M. Kluck. 2011. Molecular biology of Bax and Bak activation and action. *Biochim. Biophys. Acta.* 1813:521–531.
14. Leber, B., J. Lin, and D. W. Andrews. 2010. Still embedded together binding to membranes regulates Bcl-2 protein interactions. *Oncogene.* 29:5221–5230.
15. Antonsson, B., F. Conti, …, J. C. Martinou. 1997. Inhibition of Bax channel-forming activity by Bcl-2. *Science.* 277:370–372.
16. Schlesinger, P. H., A. Gross, …, S. J. Korsmeyer. 1997. Comparison of the ion channel characteristics of proapoptotic BAX and antiapoptotic BCL-2. *Proc. Natl. Acad. Sci. USA.* 94:11357–11362.
17. Schlesinger, P. H., and M. Saito. 2006. The Bax pore in liposomes, Biophysics. *Cell Death Differ.* 13:1403–1408.
18. Basañez, G., A. Nechushtan, …, R. J. Youle. 1999. Bax, but not Bcl-xL, decreases the lifetime of planar phospholipid bilayer membranes at subnanomolar concentrations. *Proc. Natl. Acad. Sci. USA.* 96:5492–5497.
19. Jonas, E. A., J. M. Hardwick, and L. K. Kaczmarek. 2005. Actions of BAX on mitochondrial channel activity and on synaptic transmission. *Antioxid. Redox Signal.* 7:1092–1100.
20. Martinez-Caballero, S., L. M. Dejean, …, K. W. Kinnally. 2009. Assembly of the mitochondrial apoptosis-induced channel, MAC. *J. Biol. Chem.* 284:12235–12245.
21. Kagawa, Y., and E. Racker. 1971. Partial resolution of the enzymes catalyzing oxidative phosphorylation. *J. Biol. Chem.* 246:5477–5487.
22. Suzuki, M., R. J. Youle, and N. Tjandra. 2000. Structure of Bax: coregulation of dimer formation and intracellular localization. *Cell.* 103:645–654.
23. Ganesan, V., M. N. Perera, …, M. Colombini. 2010. Ceramide and activated Bax act synergistically to permeabilize the mitochondrial outer membrane. *Apoptosis.* 15:553–562.
24. Brustovetsky, T., T. Li, …, N. Brustovetsky. 2010. BAX insertion, oligomerization, and outer membrane permeabilization in brain mitochondria: role of permeability transition and SH-redox regulation. *Biochim. Biophys. Acta.* 1797:1795–1806.
25. Montal, M., and P. Mueller. 1972. Formation of bimolecular membranes from lipid monolayers and a study of their electrical properties. *Proc. Natl. Acad. Sci. USA.* 69:3561–3566.
26. Colombini, M. 1987. Characterization of channels isolated from plant mitochondria. *Methods Enzymol.* 148:465–475.
27. Goldman, D. E. 1943. Potential, impedance, and rectification in membranes. *J. Gen. Physiol.* 27:37–60.
28. Hodgkin, A. L., and B. Katz. 1949. The effect of sodium ions on the electrical activity of giant axon of the squid. *J. Physiol.* 108:37–77.
29. Hall, J. E. 1975. Access resistance of a small circular pore. *J. Gen. Physiol.* 66:531–532.
30. Xu, X., and M. Colombini. 1996. Self-catalyzed insertion of proteins into phospholipid membranes. *J. Biol. Chem.* 271:23675–23682.
31. Petersheim, M., and J. Sun. 1989. On the coordination of La^{3+} by phosphatidylserine. *Biophys. J.* 55:631–636.
32. Brown, M., and J. Seelig. 1977. Ion-induced changes in head group conformation of lecithin bilayers. *Nature.* 269:721–723.
33. Seelig, J., P. M. Macdonald, and P. G. Scherer. 1987. Phospholipid head groups as sensors of electric charge in membranes. *Biochemistry.* 26:7535–7541.
34. Tanaka, T., Y. Tamba, …, M. Yamazaki. 2002. La(3+) and Gd(3+) induce shape change of giant unilamellar vesicles of phosphatidylcholine. *Biochim. Biophys. Acta.* 1564:173–182.
35. Ermakov, Y. A., K. Kamaraju, …, S. Sukharev. 2010. Gadolinium ions block mechanosensitive channels by altering the packing and lateral pressure of anionic lipids. *Biophys. J.* 98:1018–1027.
36. Pavlov, E. V., M. Priault, …, K. W. Kinnally. 2001. A novel, high conductance channel of mitochondria linked to apoptosis in mammalian cells and Bax expression in yeast. *J. Cell Biol.* 155:725–731.
37. Annis, M. G., E. L. Soucie, …, D. W. Andrews. 2005. Bax forms multispanning monomers that oligomerize to permeabilize membranes during apoptosis. *EMBO J.* 24:2096–2103.
38. García-Sáez, A. J., I. Mingarro, …, J. Salgado. 2004. Membrane-insertion fragments of Bcl-xL, Bax, and Bid. *Biochemistry.* 43:10930–10943.
39. Saito, M., S. J. Korsmeyer, and P. H. Schlesinger. 2000. BAX-dependent transport of cytochrome *c* reconstituted in pure liposomes. *Nat. Cell Biol.* 2:553–555.
40. Nechushtan, A., C. L. Smith, …, R. J. Youle. 2001. Bax and Bak coalesce into novel mitochondria-associated clusters during apoptosis. *J. Cell Biol.* 153:1265–1276.
41. Ross, K., T. Rudel, and V. Kozjak-Pavlovic. 2009. TOM-independent complex formation of Bax and Bak in mammalian mitochondria during TNFalpha-induced apoptosis. *Cell Death Differ.* 16:697–707.
42. Colombini, M. 2004. VDAC: the channel at the interface between mitochondria and the cytosol. *Mol. Cell. Biochem.* 256-257:107–115.
43. Lemeshko, V. V. 2002. Model of the outer membrane potential generation by the inner membrane of mitochondria. *Biophys. J.* 82:684–692.
44. Porcelli, A. M., A. Ghelli, …, M. Rugolo. 2005. pH difference across the outer mitochondrial membrane measured with a green fluorescent protein mutant. *Biochem. Biophys. Res. Commun.* 326:799–804.
45. Ausili, A., A. Torrecillas, …, J. C. Gómez-Fernández. 2008. The interaction of the Bax C-terminal domain with negatively charged lipids modifies the secondary structure and changes its way of insertion into membranes. *J. Struct. Biol.* 164:146–152.